Available online at www.sciencedirect.com
ScienceDirect
Advances in Water Resources 30 (2007) 2061–2071
Advances in Water Resources
www.elsevier.com/locate/advwatres

Propagation of uncertainty from rainfall to runoff: A case study with a stochastic rainfall generator

S. Gabellani [a], G. Boni [a,b], L. Ferraris [a,b], J. von Hardenberg [a,c,*], A. Provenzale [a,c]

[a] CIMA, Centro di Ricerca Interuniversitario in Monitoraggio Ambientale, Universities of Genoa and of Basilicata, Savona, Italy
[b] DIST, Dipartimento di Informatica Sistemistica e Telematica, University of Genoa, Genoa, Italy
[c] ISAC-CNR, Istituto di Scienze dell'Atmosfera e del Clima, Torino, Italy

Received 19 October 2005; received in revised form 14 July 2006; accepted 5 November 2006
Available online 5 April 2007

Abstract

We explore the impact of uncertainties in the spatial–temporal distribution of rainfall on the prediction of peak discharge in a typical mountain basin. To this end, we use a stochastic generator previously developed for rainfall downscaling, and we estimate the basin response by adopting a semi-distributed hydrological model. The results of the analysis provide information on the minimum rainfall resolution needed for operational flood forecasting, and confirm the sensitivity of peak discharge estimates to errors in the determination of the power spectrum of the precipitation field.

Keywords: Uncertainty propagation; Stochastic rainfall models; Rainfall–runoff processes

1. Introduction

The spatial and temporal distribution of rainfall plays an important role in determining the hydrological response of river basins, particularly for catchments characterized by a Hortonian runoff mechanism. For this reason, uncertainties in the statistical properties of rainfall can be a significant source of error in flood forecast procedures [1,5–7,15,16,18,20–22,26,27,29,30,32–34].

This problem becomes critical in small mountain catchments and urban areas, where flood prediction requires the forecast of the precipitation field down to scales of a few square kilometers and tens of minutes [8,10,28]. In such situations, it becomes necessary to quantify how uncertainties in the statistical properties of the forecasted rain fields affect estimates of river runoff and peak discharge.

Along these lines, in this work we focus on the following questions: (1) what is the minimum scale below which the detailed distribution of rainfall peaks does not significantly affect basin response, and (2) what is the impact of uncertainties in the correlation structure of the precipitation field, and, more specifically, of an uncorrect estimate of its logarithmic spectral slopes. To address these issues, we generate synthetic precipitation fields with given statistical properties, and we use them as inputs to a semi-distributed rainfall–runoff model to generate peak flow estimates. We then assess how the peak discharge estimates respond to variations in the statistical properties of rainfall.

The rest of this paper proceeds as follows. In Section 2 we describe in some detail the stochastic model *RainFARM* used to generate the synthetic rainfall fields [24], and the rainfall–runoff model *DRiFt* used to generate peak discharge estimates [14]. Section 3 discusses the sensitivity of peak discharge estimates to uncertainties in the spatial–temporal distribution of rainfall, and Section 4 considers the effects of varying the average slope of the

* Corresponding author. Address: ISAC-CNR, Istituto di Scienze dell'Atmosfera e del Clima, Torino, Italy.
E-mail address: j.vonhardenberg@isac.cnr.it (J. von Hardenberg).

0309-1708/$ - see front matter © 2007 Elsevier Ltd. All rights reserved.
doi:10.1016/j.advwatres.2006.11.015

rainfall power spectra. Section 5 gives conclusions and perspectives.

2. Methodology

The methodology of this study is based on generating ensembles of spatial–temporal rainfall events by a stochastic downscaling model, and then using the fields as inputs to a semi-distributed rainfall–runoff model. We first assess the sensitivity of the basin response to variations in the spatial and temporal distribution of rainfall, associated with different choices of the set of Fourier phases, for a fixed shape of the power spectrum. Subsequently, we study the influence of variations in the linear correlations of the rainfall fields, obtained by modifying the spectral slopes of the simulated rain fields.

In the following, we focus on the Tanaro basin in North-Western Italy, an area which has been subject to intense investigation in past years. The Tanaro source is in the Ligurian Alps, close to the Marguareis mountains. At its junction with the Po river, the Tanaro drains about 8000 km^2, 500 km^2 of which are in mountainous terrain. Major tributaries are the Stura di Demonte (1430 km^2), Alto Tanaro (1840 km^2), Belbo (480 km^2), Bormida (1640 km^2) and Orba (840 km^2). Morphological variability allows for the identification of three main zones with a characteristic behavior. The mountain part has an average slope of 6%, very steep catchments and deep river beds; the mild part has an average slope of 1%, shallower river beds and mildly steep catchments; finally, the alluvial part is characterized by very low slope values. The Tanaro is characterized by relevant flood events in spring and autumn and dry periods during summer.

Here, we consider in detail two examples: the Tanaro closed at the town of Alba, with area of 3415 km^2 and time of concentration of about 16 h, and the Orba closed at the village of Casalcermelli, with area of 840 km^2 and time of concentration of about 8 h.

2.1. Generation of synthetic rain fields

The rainfall fields used in this work are generated by the *RainFARM* model, which has been shown to correctly reproduce the small-scale statistical properties of intense rainfall events [24]. This stochastic rainfall model is based on nonlinearly filtering a stochastic field obtained by an autoregressive linear process [4]. In its current implementation, the model generates the rain fields by first taking the inverse Fourier transform of a spatial–temporal power-law power spectrum with random Fourier phases (a procedure that leads to a stochastic Gaussian field [23,11]), and then taking the exponential of the Gaussian field [12]. A small precipitation threshold can be further introduced, to generate pixels with strictly null precipitation. More specifically, each stochastic realization of the rainfall field, $r(x,y,t)$, where (x,y) are the spatial coordinates and t is time, is obtained as

$$r(x,y,t) = C\exp[g(x,y,t)]\theta(r-r_0), \tag{1}$$

where r_0 is a (very small) precipitation threshold, $\theta(r-r_0)=1$ for $r \geqslant r_0$ and $\theta = 0$ for $r < r_0$, and

$$g(x,y,t) = \int \mathrm{d}x\mathrm{d}y\mathrm{d}t[P(k_x,k_y,\omega)]^{1/2}\exp[k_x x + k_y y - \omega t + \phi(k_x,k_y,\omega)], \tag{2}$$

where (k_x,k_y) are the spatial wavenumbers and ω is the angular frequency. The power spectrum P is given by

$$P(k_x,k_y,\omega) \propto \frac{1}{(k_x^2+k_y^2)^{\alpha/2}|\omega|^{\beta}} \tag{3}$$

and $\phi(k_x,k_y,\omega)$ are random Fourier phases uniformly distributed in $[0,2\pi)$. The field g is normalized to have zero mean and unit variance.

The free parameters of the model are the logarithmic spectral slopes in space and time, α and β, the constant C that fixes the total rainfall volume during the event, and the precipitation threshold r_0 (in fact, this latter can be set to zero without qualitatively changing the results). In the following, the *RainFARM* model is used to generate rainfall events with given statistical properties in two spatial domains that contain the catchments under study, as shown in Fig. 1. The domains have side $L_0 = 128$ km and spatial resolution $\Delta x = 1$ km. The rainfall events have duration $T_0 = 32$ h and temporal resolution $\Delta t = 30$ min.

2.2. The hydrological model

The response of the basins to a precipitation event is simulated by the semi-distributed rainfall–runoff model *DRiFt* (Discharge River Forecast) described in [13,14]. This model has been developed for small and medium size basins in a semi-arid climate, in which orographic convective precipitation is the main source of flood events and where the Horton saturation mechanism is predominant. The model is semi-distributed, partial, and event-based, and it takes into account the morphology of the basin. The model accepts as inputs a set of spatially distributed soil-type and soil-use fields and a spatial–temporal rainfall field, and it gives the discharge response at a section of the basin. The horizontal grid used to discretize the catchments has a resolution of 250×250 m. The parameters of the *DRiFt* model (hillslope velocity, channel velocity and geomorphologic filter) do not change in the different numerical simulations discussed in the following. Either the *SCS-CN* [19,31] or a modified Horton method [2,3,17] can be used to compute infiltration.

The initial conditions on soil moisture in the *DRiFt* model are expressed in terms of the antecedent moisture conditions (AMC), that measure the wetness of the soil surface and the amount of moisture available in the soil profile before the start of a storm. In the following, we consider the case of AMC-I (dry soil initial conditions) and *SCS-CN* infiltration scheme. We repeated some of the numerical experiments using different initial conditions and infiltration schemes, obtaining analogous results.

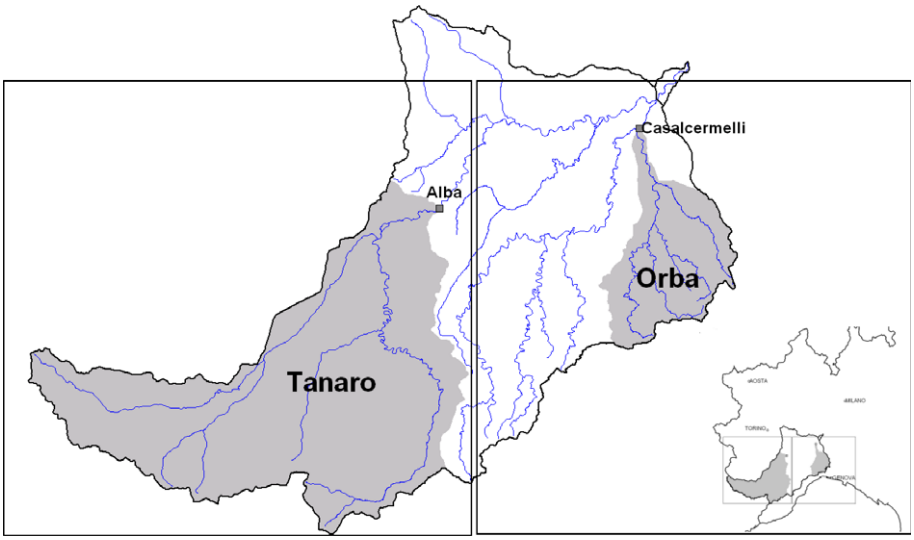

Fig. 1. Spatial domains of the simulated rain fields. The solid line marks the perimeter of the Tanaro basin closed at the confluence with the Po river. The shaded areas indicate the two basins considered in this study. The inset in lower right corner reports a schematic map of Northern Italy with the geographical position of the Tanaro basin.

3. Uncertainties in the spatial–temporal distribution of rainfall

To estimate the sensitivity of basin response to the spatial–temporal distribution of rainfall, we simulated a large number of rainfall events with the same power spectrum but with a different choice of the set of Fourier phases. In this way, the statistical properties and the visual appearance of the precipitation fields are the same for the different events, and only the localization of the rainfall peaks inside the basin vary from one realization to another [24].

The spectra have logarithmic slopes $\alpha = 1.7$ and $\beta = 1.2$, consistent with the spectral properties of intense events in this area [9,25]. To avoid differences in the hydrological response due to volumetric effects, only an ensemble of 1000 events that have approximately the same cumulated precipitation volume on the basin and on the duration of the event, with differences of at most 1%, are selected for the analysis.[1] In this way, volume effects become negligible and one can identify the effects due to variations in the spatial and temporal distribution of rainfall. Fig. 2 shows, as an example, two snapshots of two different precipitation fields extracted from the ensemble of simulated events.

Fig. 3 shows examples, for the Tanaro and Orba basins, of 100 discharge time series, $Q(t)$, extracted from the ensemble of 1000 rainfall–runoff events. Even though the events have similar rainfall volumes, the differences in peak discharge values are quite impressive. In the case of the Tanaro basin, Fig. 4a shows the distribution of peak discharge values, Q^P, normalized by their mean value, Q^P_m. Panel (a) is for the configuration described above and panel (b) is for a case when infiltration is set to zero. The lower two panels (c and d), show for comparison the distribution that would be obtained for uniform rainfall, and provide an estimate of the residual volumetric effects associated with the 1% volume tolerance in the selection of the events. Compared to a volumetric difference of at most 1%, the spatial and temporal variability of rainfall is responsible for a dispersion of the peak discharge of 20–25%. As it could have been expected, the dispersion is slightly lower if the effects of infiltration are neglected.

The case with no infiltration is especially interesting because it helps drawing a distinction between runoff production and runoff concentration. Since the rainfall volume over the basin is approximately the same for the different events, when infiltration is set to zero the differences in runoff production reflect the difference in rainfall volume, of the order of 1%. On the other hand, Fig. 3b indicates differences in peak discharge of the order of 20%, which are produced by differences in runoff concentration for the different events, associated with the different spatial–temporal distribution of precipitation intensity. It is intriguing that even for a similar total rainfall volume during the event, and for similar statistical properties of the precipitation, the differences in the details of the rainfall peak distribution

[1] The simple procedure of re-normalizing precipitation fields with widely different volumes to have a fixed volume over the basin cannot be applied. This is because the precipitation fields (both the real ones and those generated by the *RainFARM*) have multifractal properties, which are associated with a different scaling behavior of peaks with different intensity. Thus, amplifying a low-precipitation portion of a field leads to a field that can have different statistical properties than a field that originally had large intensity peaks in the area of interest. For this reason, we prefer to generate many fields and select only those which have approximately the same volume over the basin of interest. The selected volume represents a typical intense precipitation event in this geographical area. Once the fields have been selected in this way, one can then safely normalize them to have exactly the same volume in cases where this is required.

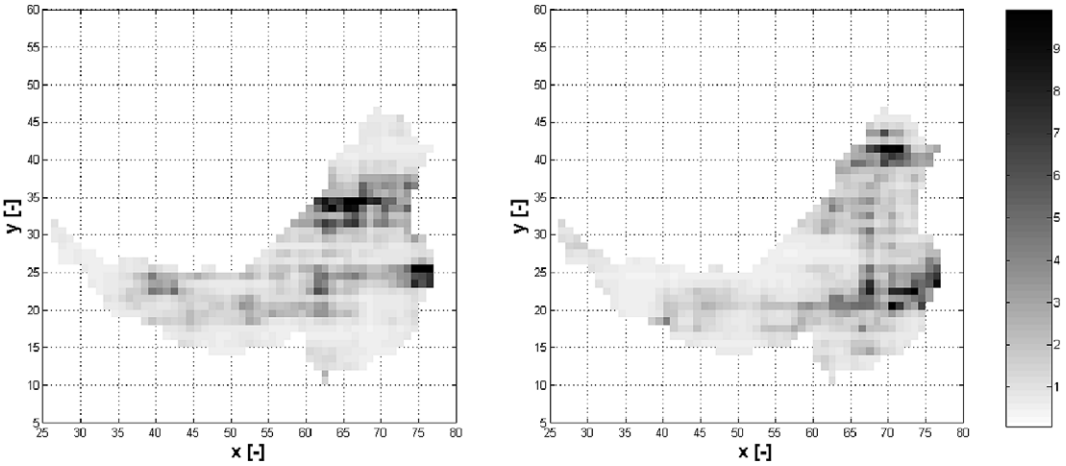

Fig. 2. Two example precipitation fields extracted from the ensemble of 1000 fields with similar volume over the Tanaro basin, generated by the *RainFARM* procedure. Logarithmic spectral slopes are $\alpha = 1.7$ and $\beta = 1.2$. The gray scale indicates precipitation [mm] cumulated over $\Delta t = 30$ min.

inside the basin can lead to such large variations in peak discharge.

In the case with infiltration, the effects of runoff concentration are augmented by differences in runoff production due to different infiltration histories of the events. However, this effect is rather small and it leads to differences in peak discharge which are not much larger than those observed with no infiltration. Thus, the main mechanism responsible for the variability of peak discharge in our model is associated with differences in runoff concentration.

3.1. Effects of the scale of uncertainty

Given that variations in the Fourier phases can lead to a different spatial–temporal distribution of rainfall peaks and to a different basin response, here we want to determine what is the scale below which uncertainties in the detailed spatial and temporal distribution of rainfall do not affect peak discharge estimates.

To address this issue, we consider an ensemble of random perturbations, either in space or in time, to a reference event. We then asses the sensitivity of the basin response to the scale of the perturbation. The reference event has logarithmic spectral slopes $\alpha = 1.7$ and $\beta = 1.2$ and a given set of Fourier phases. We call V_0 the cumulated rainfall over the basin and Q_0^P the peak discharge of the reference event. We generate ensembles of 1000 perturbed events by different randomizations of the Fourier phases below a given scale [12]. Practically, this is obtained by substituting the original Fourier phases with randomly-distributed phases for all wavenumbers $k_x > 2\pi/L$, $k_y > 2\pi/L$ or all frequencies $\omega > 2\pi/T$, where L and T are the maximum space and time perturbation scales respectively. As the scale of the perturbation decreases, differences in the spatial–temporal structure of the perturbed events become smaller and the perturbed rain fields become closer to the reference event.

The detailed flow-chart of a typical numerical experiment is as follows:

- Selection of a reference event → Computation of V_0 and Q_0^P.
- Perturbation of the reference event by randomizing either:
  - the spatial Fourier phases below the scale L, or
  - the temporal Fourier phases below the scale T.
- Selection of 1000 perturbed events so that their volume, V_{pert}, cumulated over the basin and the duration of the event, differs by less than 0.5% from V_0.
- Normalization of the perturbed events to have exactly the reference volume on the basin.
- Estimate of the distribution of normalized peak discharge values obtained from the ensemble of perturbed events,

$$\frac{Q^P_{\text{pert}} - Q^P_0}{Q^P_0},$$

where Q^P_{pert} is the peak discharge of the perturbed event.

The distribution of peak discharge values for the perturbed events is shown in Fig. 5 for the Tanaro basin, for different values of L/D where D is the square root of the basin area. The results for the Orba basin, not shown, are similar. The smaller is the scale below which the events are perturbed, the smaller is the spread of the peak distribution. The influence of the temporal distribution of rainfall at different scales has been similarly analyzed by perturbing the temporal Fourier phases of the reference event below a given time scale T, obtaining analogous results.

Fig. 6 shows the values of the r.m.s. spread of the distribution (square root of the variance) for spatial perturbations (upper panel) and for temporal perturbations (lower panel), as a function of the maximum perturbation scales, L and T, normalized to the characteristic basin scales, D and T_c, where T_c is the time of concentration.

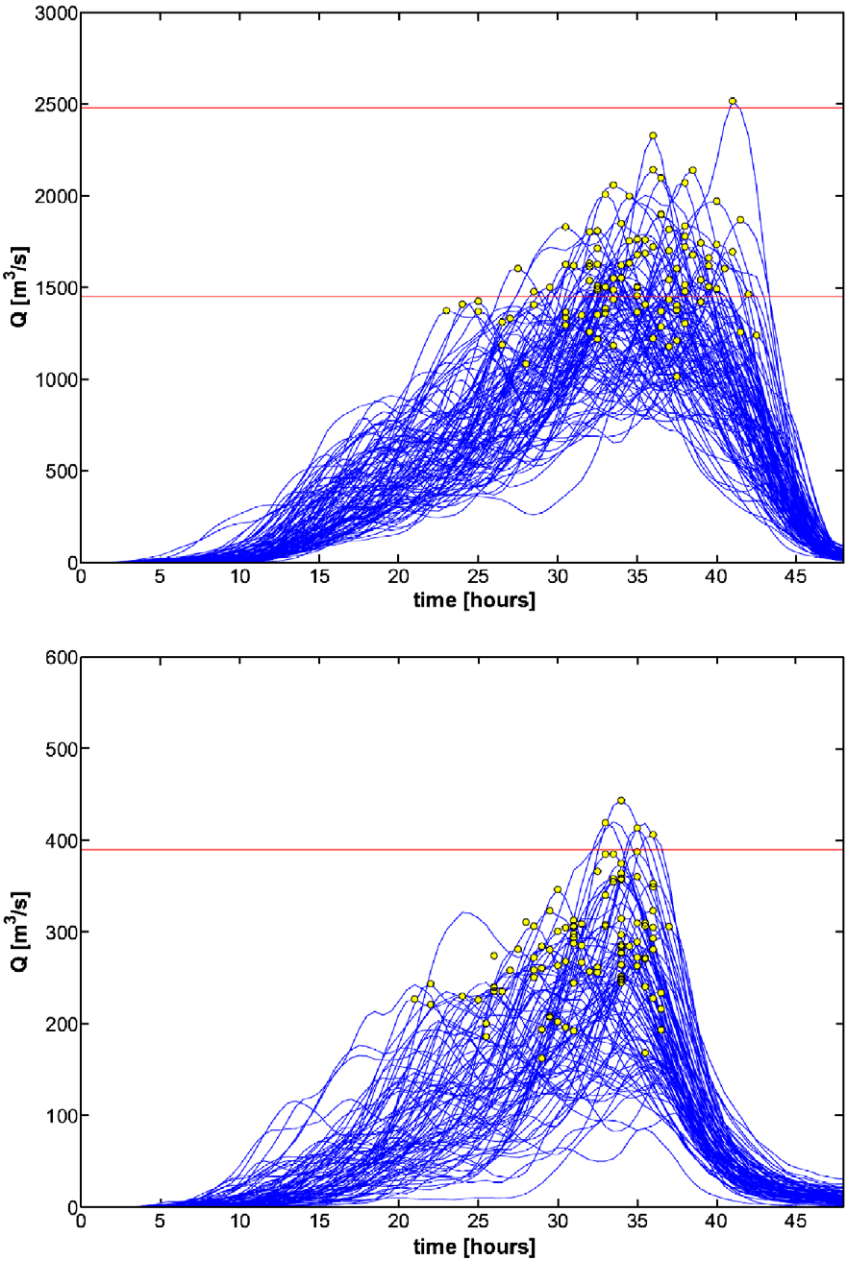

Fig. 3. A set of 100 example hydrographs for the Tanaro closed at Alba (upper panel) and for the Orba closed at Casalcermelli (lower panel). The hydrographs for each basin are generated by rainfall events that differs by at most 1% in the cumulated rainfall volume on the basin and on the duration of the event. Horizontal lines indicate different warning levels for the two basins. The open circles mark the peak discharge for each hydrograph.

The spread of the peak discharge distribution grows with the scale of the perturbation, and it is consistent with zero spread when the scale of the perturbation vanishes. For temporal perturbations, one observes a tendency towards saturation in the spread of peak discharge values when $T \approx T_c$. This confirms the importance of runoff concentration processes, and is consistent with the fact that the detailed distribution of rainfall on time scales longer than the time of concentration does not substantially increase the variability of peak discharge. Conversely, no saturation at $L \approx D$ is apparent in the case of spatial perturbations, suggesting that also long-wave components in the spatial rainfall distribution can influence the basin response.

The results shown in Fig. 6 indicate that a well-defined sensitivity scale of the basin does not exist, at least for the rainfall–runoff model used here. However, we can operationally define a sensitivity scale by fixing an uncertainty threshold on the peak discharge. For example, neglecting the spatial variability of rain fields below a scale $L/D \approx 0.2$ (corresponding to about 11 km for the Tanaro closed at Alba and to 6 km for the Orba closed at Casalcermelli) leads to a r.m.s. uncertainty in the peak estimate of about 5%. In the time domain, neglecting the temporal

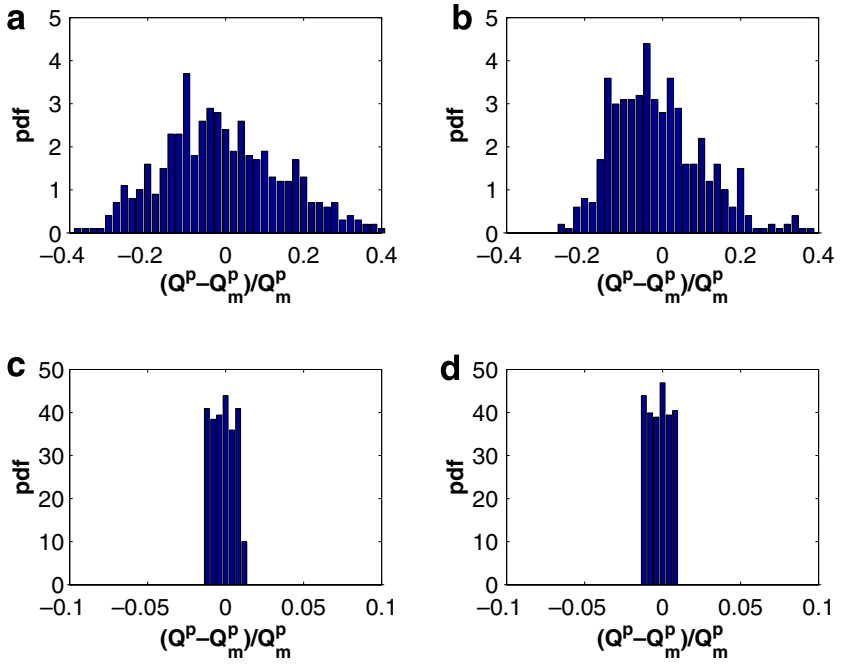

Fig. 4. (a) Distribution of normalized peak discharge values, $(Q^P - Q^P_m)/Q^P_m$, from a set of 1000 rainfall events with the same power spectrum for the Tanaro basin closed at Alba. The rainfall volumes (cumulated over the basin and on the duration of the event) differ by at most 1% from each other. (b) Same as (a) but neglecting infiltration in the rainfall–runoff model. (c) Same as (a), but for rainfall events which are uniform in space and time. (d) Same as (c), but neglecting infiltration. Note the different horizontal scale in the upper and lower panels.

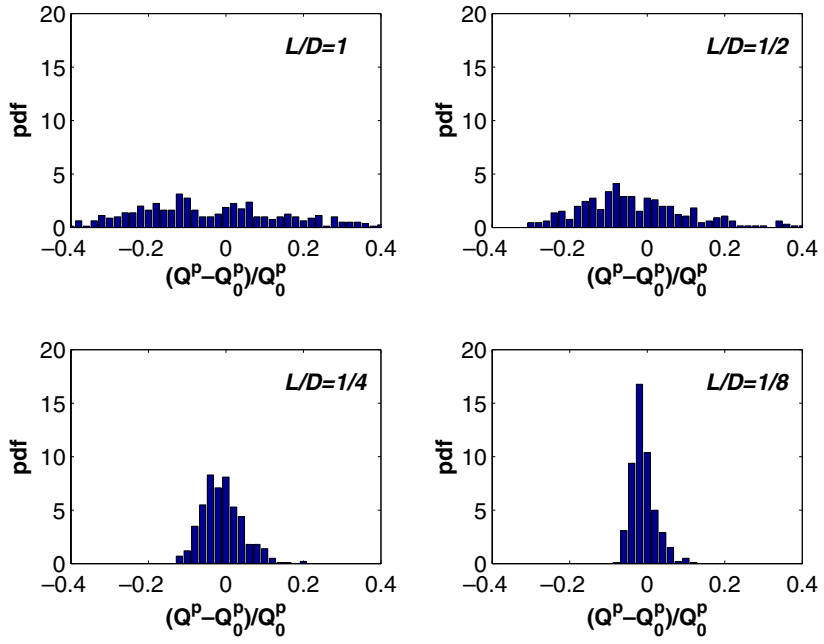

Fig. 5. Distribution of normalized peak discharge values obtained by perturbing the spatial distribution of rainfall at different scales; case for the Tanaro basin closed at Alba.

variability of rainfall below a scale $T/T_c = 0.2$ (corresponding to about 3 h for the Tanaro closed at Alba and to 1.5 h for the Orba closed at Casalcermelli) leads to a r.m.s. uncertainty on the peak discharge of about 5%. In both cases, we assumed that the precipitation volume over the basin had been predicted correctly.

4. Influence of the rainfall correlation structure

Here we use the *RainFARM* model to generate an ensemble of 1000 reference events with the same spectral slopes ($\alpha = 1.7, \beta = 1.2$) but with different Fourier phases and different cumulated volumes over the basin. For each

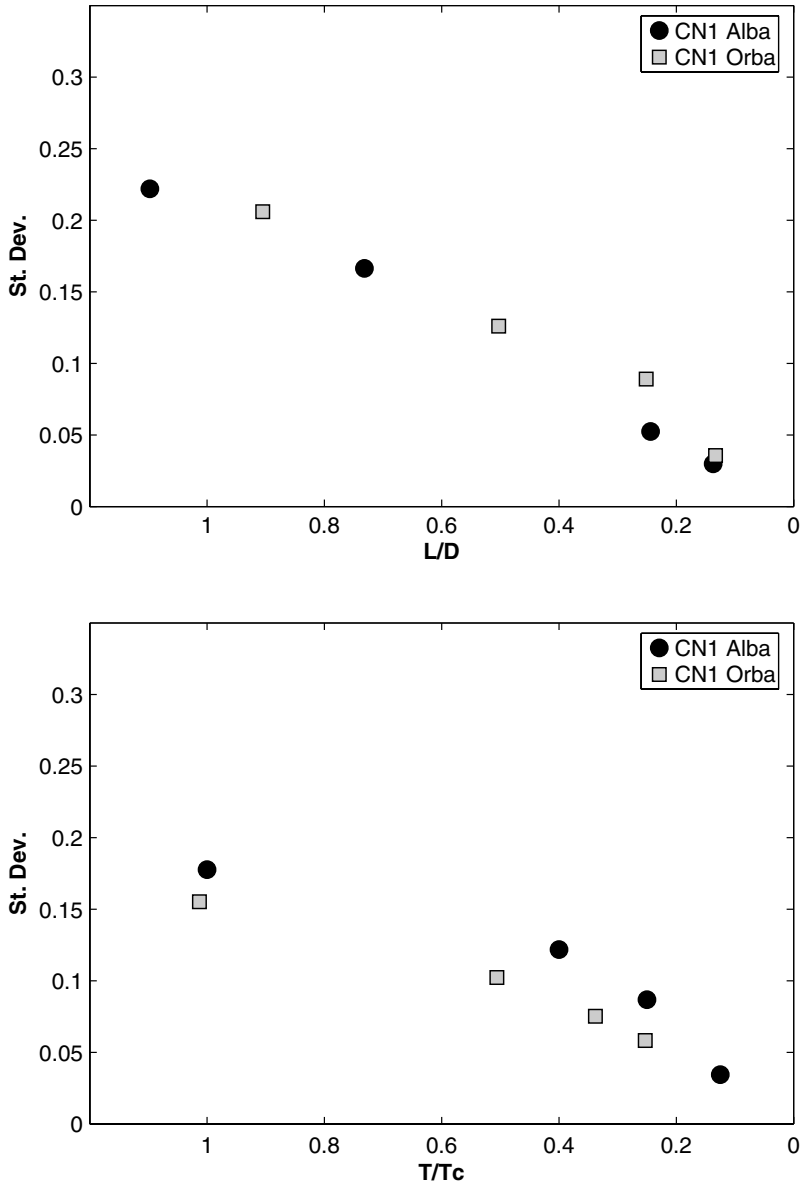

Fig. 6. R.m.s. spread of the peak discharge distribution of the perturbed events versus the maximum spatial scale of the perturbation, for the Tanaro basin closed at Alba and for the Orba closed at Casalcermelli. The upper panel is for spatial perturbations and the lower panel is for temporal perturbations.

of these events, we create a small ensemble of perturbed events with the same Fourier phases and rainfall volume of the corresponding reference event, but with different spectral slopes either in space or in time. Thus, the reference and perturbed events differ only in the strength of the second-order spatial or temporal autocorrelations, which are determined by the spectral slopes. Larger spectral slopes lead to more autocorrelated events while smaller slopes lead to less autocorrelated fields, as illustrated in Fig. 7. Note that, in principle, changing the spectral slopes can lead to changes in the rainfall volume over the basin. We verified that the volume changes induced by the perturbations in the spectral slopes do not exceed 5%, and we thus opted for re-normalizing the perturbed rain fields to have exactly the same volume as the corresponding reference event.

Fig. 8 shows the peak discharges of the perturbed events, versus the peaks of the corresponding reference events, for the whole ensemble of 1000 rainfall events on the Tanaro basin closed at Alba. Only the spatial spectral slopes have been modified, and the perturbed events have spectral slopes $\beta = 1.2$ and $\alpha = 1.2$ (upper left panel), $\alpha = 1.4$ (upper right), $\alpha = 1.9$ (lower left), and $\alpha = 2.1$ (lower right). The results for the Orba basin (not shown) are similar.

The modification of the temporal correlations has a similar effect. Fig. 9 shows the peak discharges of the perturbed events, versus the peaks of the corresponding reference events, when only the temporal spectral slopes are modified. The perturbed events have spectral slopes $\alpha = 1.7$ and $\beta = 1$ (upper left panel), $\beta = 1.4$ (upper right), $\beta = 1.6$ (lower left) and $\beta = 1.8$ (lower left). Again, the results for the Orba basin are similar.

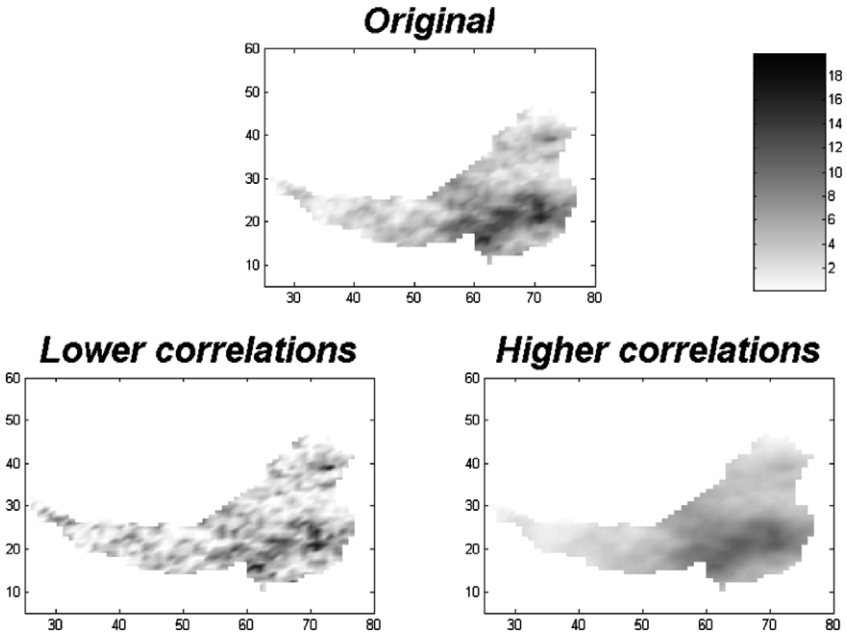

Fig. 7. Snapshots of the rainfall fields obtained by modifying the logarithmic slopes of the spatial power spectrum. The original field has spectral slope $\alpha = 1.7$, the lower-left field has $\alpha = 0.7$ and the lower-right field has $\alpha = 2.7$. The gray scale indicates precipitation [mm] cumulated over $\Delta t = 30$ min.

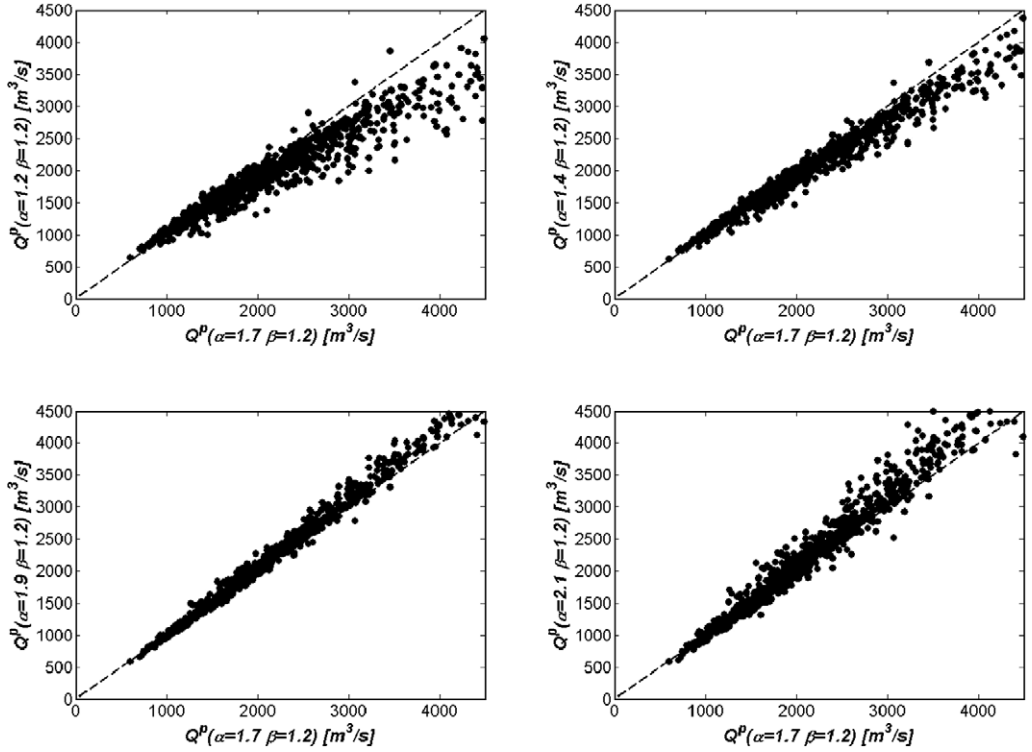

Fig. 8. Discharge peaks of the events, obtained by perturbing the spatial spectral slopes, versus the peaks of the reference events for the Tanaro closed at Alba. The reference events have logarithmic spectral slopes $\alpha = 1.7$ and $\beta = 1.2$. The perturbed events have the same temporal spectral slope but $\alpha = 1.2$ (upper left panel), $\alpha = 1.4$ (upper right), $\alpha = 1.9$ (lower left), and $\alpha = 2.1$ (lower right).

These two figures indicate that more correlated events, at equal values of rainfall volume and Fourier phases, lead to larger peak discharges. This is especially evident for large peak discharge, where the dependence on the spectral slope of the event is stronger. To further verify this inference, we have considered a case where the reference rain field has been shuffled over the basin, either in space or in time, thus generating a perturbed rain field with a white power spectrum but exactly the same rainfall volume. In this case, the peak discharge that is generated is much lower than

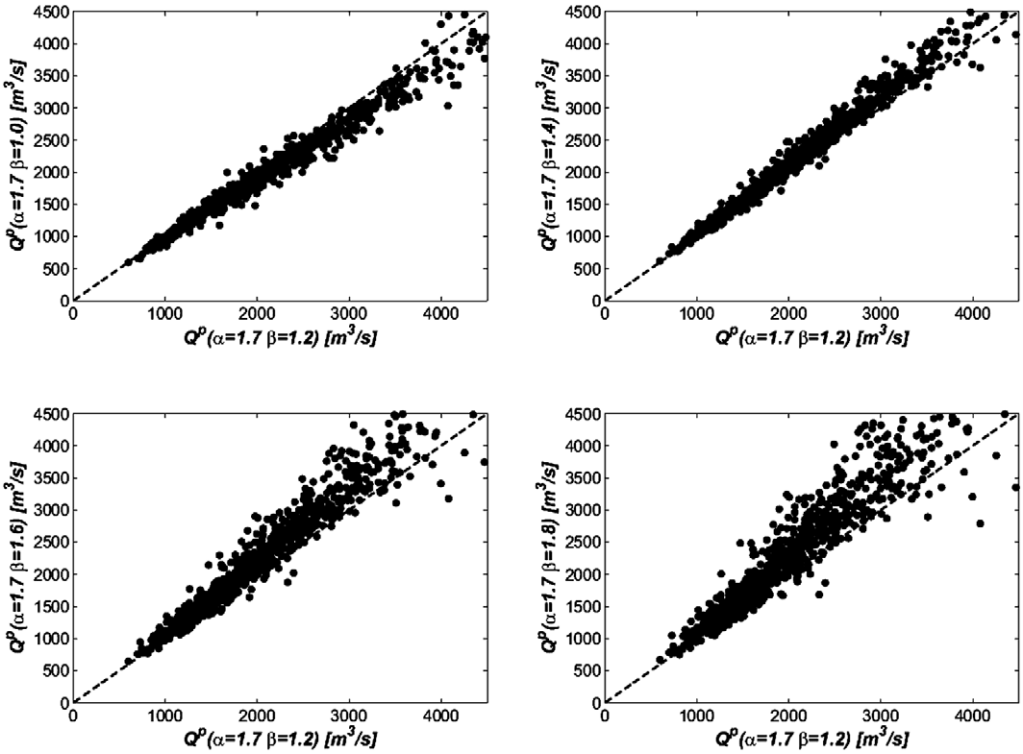

Fig. 9. Discharge peaks of the events, obtained by perturbing the temporal spectral slopes, versus the peaks of the reference events for the Tanaro closed at Alba. The reference events have logarithmic spectral slopes $\alpha = 1.7$ and $\beta = 1.2$. The perturbed events have the same spatial spectral slope but $\beta = 1$ (upper left panel), $\beta = 1.4$ (upper right), $\beta = 1.6$ (lower left), and $\beta = 1.8$ (lower right).

the value associated with the field with the original autocorrelation structure. This confirms that the spectral slopes of the rain fields play an essential role in determining the hydrological response, and implies that forecasts that underestimate the spatial or temporal autocorrelation of the rain field lead to a potential underestimate of the intensity of peak discharge.

The correlation structure of the rainfall field, as indicated by the logarithmic spectral slope, is related to the intensity of the precipitation peaks. The steeper the slope is, the fewer, the more intense and the more correlated are the individual precipitation peaks. The process of runoff concentration is sensitive to the intensity and to the mutual correlation of the individual rainfall peaks inside the basin: for a few, highly correlated and intense peaks, the probability of large peak discharges becomes higher than for many smaller peaks, even for the same total rainfall volume. When the spectral slope is underestimated, the basin response is correspondingly underestimated.

5. Discussion and conclusions

Uncertainties in the small-scale statistical properties of forecasted rain fields propagate along the rainfall–runoff chain and affect the prediction of peak discharge. In this work we analyzed numerically, for the specific cases of the Tanaro and Orba basins in North-Western Italy, the sensitivity of peak discharge estimates to uncertainties in the spatial and temporal statistics of rainfall. To this end, we used the stochastic *RainFARM* model to generate synthetic rain fields which were used as input to the *DRiFt* rainfall–runoff model.

In the course of the analysis, we tested the sensitivity of peak discharge estimates to the spatial and temporal localization of the rain structures, as described by the Fourier phases of the rain field, and to the strength of the rain autocorrelation in space and time, as measured by the logarithmic slope of the power spectra. We discussed explicitly the results obtained for the SCS-CN method with dry-soil initial conditions (AMC-I). Preliminary explorations with different antecedent soil moisture conditions and/or different infiltration schemes provided analogous results.

For rainfall fields with approximately the same cumulated precipitation volume over the basin and the same autocorrelation structure, but with different spatial–temporal distribution of rainfall peaks inside the basin, we observe differences in peak discharge estimates of up to 25%. Even when the correct rainfall volume is forecasted, an error in the localization of the rain cells at scales smaller than the basin size can lead to serious errors in peak discharge estimates. Of course, uncertainties at scales larger than those of the basin lead to even larger errors. The sensitivity of basin response to the precise localization of rainfall peaks is mainly due to the process of runoff concentration, as indicated by the results obtained when soil infiltration is set to zero.

As a further step, we investigated what are the spatial and temporal scales below which uncertainties in the structure of the precipitation field do not significantly affect the estimate of peak discharge. To this end, we have perturbed an ensemble of reference events by randomizing the Fourier phases below a spatial scale L or a temporal scale T, respectively smaller than the basin scale D and the basin time of concentration T_c. This exercise revealed that a well-defined sensitivity scale of the basin cannot be identified. If we use an operational definition and accept a r.m.s. uncertainty on peak discharge estimates of 5%, the results indicate that we have to resolve the precipitation field down to spatial scales of the order of $0.2\,D$ and temporal scales of about $0.2\,T_c$. For the Tanaro basin closed at Alba, this implies the need for correctly forecasting the precipitation field down to a spatial scale of about 11 km and a temporal scale of about 3 h.

Our exploration continued with the assessment of the role of spatial and temporal rainfall autocorrelations, which we perturbed by changing the logarithmic slopes of the power spectra. The results indicate that underestimating the autocorrelation of the rainfall field (i.e., predicting a lower value of the spectral slope) leads to a potential underestimate of the strength of peak discharge. This is due to the fact that rainfall fields with shallower spectral slopes are characterized by smaller and more distributed precipitation peaks, which through the runoff concentration process lead to a weaker basin response. Extreme care should thus be exercised in correctly forecasting the rainfall correlation structure.

On a final note, we comment on the generality of the results discussed in this work. The results reported here refer to a simulation study conducted with a specific choice of the rainfall and of the rainfall–runoff models. Both of these models have been shown to correctly reproduce the small-scale statistical properties of precipitation fields [24] and the peak discharge in the selected basins [14], and thus we expect the results discussed here to provide information on the behavior of the real basins. In particular, the sensitivity of basin response to the scale of perturbation is in line with empirical estimates; here we provided a quantitative assessment of the spread of peak discharge as a function of the perturbation scale. Another general aspect is the sensitivity of peak discharge to the correlation structure of rainfall, which is due to general properties of the runoff concentration process and does not depend on the specific modelling choices adopted. In any event, a full generalization of the present results requires simulation studies with other rainfall–runoff models and/or a careful – but indeed difficult – analysis of measurements from case studies.

Acknowledgement

We are grateful to the reviewers of this work for comments that greatly helped us to improve the presentation.

References

[1] Arnaud P, Bouvier C, Cisneros L, Dominguez R. Influence of rainfall spatial variability on flood prediction. J Hydrol 2002;260:216–30.
[2] Aron G. Adaptation of Horton and SCS infiltration equations to complex storms. J Irrigat Drainage Eng 1990;118:275–84.
[3] Bauer SW. A modified Horton equation during intermittent rainfall. Hydrol Sci Bull 1974;19:219–29.
[4] Bell TL. A space–time stochastic model of rainfall for satellite remote sensing studies. J Geophys Res 1987;92(D8):9631–43.
[5] Beven KJ, Hornberger GM. Assessing the effect of spatial pattern of precipitation in modeling stream flow hydrographs. Water Res Bull 1982;18:823–9.
[6] Beven KJ, Freer J. Equifinality, data assimilation, and uncertainty estimation in mechanistic modelling of complex environmental systems using the GLUE methodology. J Hydrol 2001;249:11–29.
[7] Bronstert A, Bardossy A. Uncertainty of runoff modelling at the hillslope scale due to temporal variations of rainfall intensity. Phys Chem Earth 2003;28:283–8.
[8] Castelli F. Atmosphere modelling and hydrology prediction uncertainty. In: Proc of workshop on hydrometeorology: impacts and management of extreme floods, La Colombella, Perugia, GNDCI, 1995. pp. 1779–94.
[9] Crane RK. Space–time structure of rain rate fields. J Geophys Res 1990;95:2001–20.
[10] Ferraris L, Rudari R, Siccardi F. The uncertainty in the prediction of flash floods in the northern mediterranean environment. J Hydrometeorol 2002;3:714–27.
[11] Ferraris L, Gabellani S, von Hardenberg J, Parodi U, Provenzale A, Rebora N. Revisiting multifractality in rainfall fields. J Hydrometeorol 2003;4:511–44.
[12] Ferraris L, Gabellani S, Rebora N, Provenzale A. A comparison of stochastic models for spatial rainfall downscaling. Water Resour Res 2003;39:WR002504.
[13] Giannoni F, Roth G, Rudari R. A semi-distributed rainfall–runoff model based on a geomorphologic approach. Phys Chem Earth 2000;25:665–71.
[14] Giannoni F, Roth G, Rudari R. A procedure for drainage network identification from geomorphology and its application to the prediction of the hydrologic response. Adv Water Res 2005;28:567–81.
[15] Goovaerts P. Geostatistical approaches for incorporating elevation into the spatial interpolation of rainfall. J Hydrol 2000;228:113–29.
[16] Gupta V, Waymire E. A stochastic kinematic study of subsynoptic space–time rainfall. Water Resour Res 1979;15:637–44.
[17] Horton RI. The role of infiltration in the hydrological cycle. Trans AGU 1933;14:446–60.
[18] Krajewski F, Lakshmi V, Georgakakos K, Jain S. A Monte Carlo study of rainfall sampling effect on a distributed catchment model. Water Resour Res 1991;28:1145–53.
[19] Mishra SK, Singh VP. Soil conservation service curve number (SCS-CN) methodology. Water science and technology library, vol. 42. Kluwer Academic Publishers; 2003.
[20] Morin J, Rosenfel D, Amitai E. Radar rainfall field evaluation and possible use of its high temporal and spatial resolution for hydrological purposes. J Hydrol 1995;172:275–92.
[21] Niemczynowicz J. Storm tracking using raingauge data. J Hydrol 1987;193:135–52.
[22] Ogden FL, Julien PY. Runoff model sensitivity to radar rainfall resolution. J Hydrol 1994;158:1–18.
[23] Osborne AR, Provenzale A. Finite correlation dimension for stochastic systems with power-law spectra. Physica D 1989;35:357–81.
[24] Rebora N, Ferraris L, von Hardenberg J, Provenzale A. The RainFARM: rainfall downscaling by a Filtered AutoRegressive Model. J Hydrometeorol 2006;4:724–38.
[25] Rebora N, Ferraris L, von Hardenberg J, Provenzale A. Rainfall downscaling and flood forecasting: a case study in the Mediterranean Sea. NHESS 2006;6:611–9.

[26] Shah SMS, O'Connell PE, Hosking JRM. Modeling the effects of spatial variability in rainfall on catchment response. 1. Formulation and calibration of a stochastic rainfall field model. Water Resour Res 1996;175:66–88.
[27] Shah SMS, O'Connell PE, Hosking JRM. Modeling the effects of spatial variability in rainfall on catchment response. 2. Experiments with distributed and lumped models. Water Resour Res 1996;175: 89–111.
[28] Siccardi F, Boni G, Ferraris L, Rudari R. A hydrometeorological approach for probabilistic flood forecast. J Geophys Res 2005:110. doi:10.1029/2004jd/005314.
[29] Tetzlaff D, Uhlenbrook S. Significance of spatial variability in precipitation for process-oriented modelling: results from two nested catchments using radar and ground station data. HESS 2005;9: 29–41.
[30] Troutman BM. Runoff prediction errors and bias in parameter estimation induced by spatial variability of precipitation. Water Resour Res 1983;19:791–810.
[31] USDA Soil Conservation Service. National Engineering Handbook – Section 4: Hydrology, 1972, Chapters 4–10.
[32] Wilson CB, Valdes JB, Rodriquez-Iturbe I. On the influence of the spatial distribution of rainfall on storm runoff. Water Resour Res 1979;15:321–8.
[33] Zehe E, Bloschl GN. Predictability of hydrologic response at the plot and catchment scales: Role of initial conditions. Water Resour Res 2004;40:W10202.
[34] Zehe E, Becker R, Bardossy A, Plate E. Uncertainty of simulated catchment runoff response in the presence of threshold processes: Role of initial soil moisture and precipitation. J Hydrol 2005;315: 183–202.